Contribution from the Department of Chemistry,
Florida State University, Tallahassee, Florida 32306-3006

# Factors Affecting Al–C Bond Reactivity of Tetradentate Schiff-Base Organoaluminum Complexes

Sharlene J. Dzugan and Virgil L. Goedken*

*Received January 24, 1986*

The reaction of bis(triethylaluminum), $Al_2(C_2H_5)_6$, with a variety of tetradentate Schiff-base ligands in benzene/acetonitrile solution yields ethane and the monoethylaluminum Schiff-base complexes. The ligands used include the 2:1 condensation products of salicylaldehyde with ethylenediamine, *o*-phenylenediamine, and propylenediamine (SALEN, SALOPHEN, and SALPN, respectively) and of acetylacetone with ethylenediamine (ACEN). These complexes are stable in the solid state in the absence of moisture but react with moisture and anhydrous HCl in solution to yield ethane and the corresponding hydroxoaluminum and chloroaluminum complexes, respectively. The susceptibility of these complexes to moisture in solution is dependent to a remarkable degree on the flexibility of the ligand. It is proposed that the remarkable resistance to hydrolysis, as compared with nonchelated aluminum alkyl species, is related to the high energy state of the square-planar four-coordinate $Al^{3+}$ species remaining on loss of the alkyl group. The X-ray crystal structure of $C_{18}H_{19}N_2O_2Al$ ($Al(SALEN)C_2H_5$, orthorhombic, $P2_12_12_1$, $a = 6.930$ (3) Å, $b = 10.186$ (4) Å, $c = 23.092$ (8) Å, $Z = 4$) reveals a 5-coordinate, square-pyramidal aluminum complex with an Al–C bond distance of 1.966 (7) Å. The average Al–O distance, 1.815 (15) Å, is much shorter than the Al–N distance, 2.020 (7) Å. The aluminum is displaced 0.540 Å from the least-squares plane of the ligating nitrogen and oxygen atoms, toward the ethyl group. The SALEN moiety adopts the usual "inverted umbrella" structure observed for monomeric transition-metal species.

## Introduction

Aluminum alkyls are used extensively in bimolecular industrial catalytic processes, functioning primarily as reducing agents for the transition-metal centers.[1] Aluminum alkyls are also known to form adducts with Lewis bases, resulting in decreased reactivity at the aluminum–carbon bond.[2] The coordination chemistry of alkylaluminum species with classical-type ligands, however, has received little attention.[3-5] This is probably a consequence of the hydrolysis that occurs in aqueous solution and the apparent difficulty in finding suitable $Al^{3+}$ starting reagents. Recently, macrocyclic aluminum compounds with stable aluminum carbon bonds have been isolated and characterized.[6-8] The relatively facile synthesis of these species led us to investigate the complementary reaction of aluminum alkyls with nonmacrocyclic tetradentate ligands. Since metal complexes with open-chain ligands are more susceptible to metal dissociation than those of the analogous closed-chain macrocycles,[9] these complexes are expected to be less stable. Variation of ligand properties can lend insight into those factors that stabilize the aluminum–alkyl bond.

The insertion of an aluminum ethyl species in the macrocyclic $[C_{22}H_{22}N_4]^{2-}$ complex has been shown to be a stepwise process. [See Figure 1].[7] Ionization of one of the replaceable protons results in a more stable diethylaluminum ligand complex. Complete insertion is then achieved under more forcing conditions, resulting in the loss of ethane and formation of the $Al[C_{22}H_{22}N_4]C_2H_5$ complex. In this study, the synthesis, reactivity, and characterization of the reaction of triethylaluminum with tetradentate Schiff bases has been investigated. The ligands used are shown in Figure 2. These ligands are more flexible and the coordination geometry is less constrained than for macrocyclic complexes, possibly influencing the preparation and reactivity of their aluminum complexes. Both the reactivity of the aluminum–carbon bond and the mechanisms for insertion are investigated.

A further goal of this research involves developing a better understanding of the coordination chemistry of aluminum. Transition-metal complexes of Schiff-base ligands have contributed significantly to the development of transition-metal chelate chemistry. Aluminum chelate complexes have been largely ignored because synthetic difficulties were perceived and possibly because the inert-gas neon configuration provides no interesting electronic spectra, in contrast to the rich and informative spectra obtained from transition-metal compounds. The oxophilicity of aluminum and the tendency for hydrolysis precludes the synthesis of aluminum–nitrogen bonded complexes by conventional ligand-exchange reactions. The properties of aluminum chelate complexes, once isolated, are expected to be similar to those of first-row transition metals on the basis of considerations of size and charge.[10] The ionic radius of aluminum is comparable to those of high-valent first-row transition metals, and thus aluminum should have a "good fit" into the centers of the chelating rings. A better understanding of the factors influencing the stability of aluminum–alkyl bonds may thus be directly applicable to transition-metal alkyl systems.

## Experimental Section

**Materials.** All solvents used were reagent grade and were stored over molecular sieves. Benzene was distilled over sodium. Triethylaluminum (93%) was purchased from Aldrich Chemical Co. The Schiff-base ligands were prepared by condensing salicylaldehyde or acetylacetone with the appropriate diamine.[11]

**Synthesis. $Al(SALEN)C_2H_5$.** In a typical preparation, 268 mg (1.00 mmol) of SALEN was suspended in 1.0 mL of anhydrous $CH_3CN$ and the solution deaerated with $N_2$. One milliliter of a 1.0 M $Al(C_2H_5)_3$ solution (1.00 mmol) in benzene was added via syringe through a serum cap. The reaction was highly exothermic. The reaction mixture was vented to allow the escape of the ethane produced, and then heating was continued until the volume was reduced by 50%. On cooling, pale yellow needles of the 1:1 complex were isolated.

**$Al(SALOPHEN)C_2H_5$.** This compound was prepared as above. On addition of a stoichiometric amount of $Al(C_2H_5)_3$ to the ligand, the solution immediately turned red-orange and heat and ethane were evolved. Yellow-orange needles were isolated. The rate of this reaction was found to be comparable to, but faster than, the SALEN insertion (vide infra).

**$Al(SALPN)C_2H_5$.** While the preparation of this compound followed the same procedure as that for the SALEN and SALOPHEN complexes, prolonged heating of the solution was required to achieve insertion of the $Al-C_2H_5$ moiety. Pale yellow crystals were isolated.

**$Al(ACEN)C_2H_5$.** This complex was more difficult to prepare than SALEN and SALOPHEN. In a typical preparation, 1 equiv of the $Al(C_2H_5)_3$/benzene solution was added to 1 equiv of the solid ligand via syringe through a serum cap. Ethane was evolved immediately, and a 2:1 metal to ligand complex was formed (vide infra). Aluminum alkyl

---

(1) Schmidt, F. K.; Ratovskii, G. V.; Dmitrieva, T. V.; Ivleva, I. N.; Borodko, Yu. G. *J. Organomet. Chem.* **1983**, *256*, 309 and references therein.

(2) Eisch, J. J. In *Comprehensive Organometallic Chemistry*; Wilkinson, G., Stone, F. G., Abel, E. W., Eds.; Pergamon: Oxford, England, 1982.

(3) Hurley, T. J.; Robinson, M. A.; Scruggs, J. A.; Trotz, S. I. *Inorg. Chem.* **1967**, *6*, 1310.

(4) Beachley, O. T., Jr.; Racette, K. C. *Inorg. Chem.* **1975**, *14*, 2534.

(5) Beachley, O. T., Jr.; Racette, K. C. *Inorg. Chem.* **1976**, *15*, 2110.

(6) Inoue, S.; Takada, N. *Bull. Chem. Soc. Jpn.* **1977**, *50*, 984.

(7) Goedken, V. L.; Ito, H.; Ito, T. *J. Chem. Soc., Chem. Commun.* **1984**, 1453.

(8) Goedken, V. L.; Ito, H.; Ito, T., to be submitted for publication.

(9) Cotton, F. A.; Wilkinson, G. *Advanced Inorganic Chemistry*, 4th ed.; Wiley: New York, 1978; Vol.

(10) Prewitt, C. T.; Shannon, R. D.; Rogers, D. B.; Sleight, A. W. *Inorg. Chem.* **1969**, *8*, 1985.

(11) Prasad, R. N.; Tandon, J. P. *J. Inorg. Nucl. Chem.* **1974**, *36*, 1473.

0020-1669/86/1325-2858$01.50/0

**Table I**

(A) Crystal Data

formula: $C_{18}H_{19}N_2O_2Al$
mol wt: 322.35
cryst syst: orthorhombic
space group: $P2_12_12_1$
$a$, Å: 6.930 (3)
$b$, Å: 10.186 (4)
$c$, Å: 23.092 (8)
$V$, Å$^3$: 1630.0 (11)
$Z$: 4
$d$(calcd), g·cm$^{-3}$: 1.313
cryst color: yellow
radiation (λ, Å): Mo K$\alpha$ (0.71073)
diffractometer: Enraf-Nonius CAD4

scan speed, deg·min$^{-1}$: 4
$2\theta$ scan range, deg: $2 \leq 2\theta \leq 55$
scan technique: $\theta$–$2\theta$
no. of data collcd: 1704
scan width, deg: 2.0
weighting factor: $\sigma_F = [(I + \sigma I)/Lp]^{1/2} - (I/Lp)^{1/2}$
no. of unique data: 1524
no. of unique data with $I > 2\sigma(I)$: 1427
no. of std reflcns: 3
no. of LS variables: 208
data param: 6.86
$R$, %($F_o$): 4.7
$R_w$, %($F_o$): 6.3
abs coeff, cm$^{-1}$: 1.294

(B) Positional Parameters for Al(SALEN)$C_2H_5$

| atom | $x$ | $y$ | $z$ | atom | $x$ | $y$ | $z$ |
|---|---|---|---|---|---|---|---|
| Al | 0.1021 (2) | 0.2872 (1) | 0.29304 (6) | C10 | −0.1436 (8) | 0.2085 (6) | 0.3906 (2) |
| O1 | 0.2468 (5) | 0.2284 (4) | 0.2338 (1) | C11 | 0.0203 (8) | 0.1625 (5) | 0.4222 (2) |
| O2 | 0.2222 (5) | 0.1671 (4) | 0.3396 (1) | C15 | 0.3407 (8) | 0.0705 (6) | 0.4247 (2) |
| N1 | −0.1025 (6) | 0.3354 (4) | 0.2349 (2) | C16 | 0.1932 (8) | 0.1375 (5) | 0.3940 (2) |
| N2 | −0.1402 (6) | 0.2462 (4) | 0.3388 (2) | C12 | −0.0014 (9) | 0.1267 (5) | 0.4817 (2) |
| C1 | 0.2452 (7) | 0.2533 (5) | 0.1776 (2) | C14 | 0.3111 (10) | 0.0390 (6) | 0.4829 (2) |
| C2 | 0.4067 (8) | 0.2192 (5) | 0.1442 (2) | C13 | 0.1449 (11) | 0.0688 (6) | 0.5099 (2) |
| C3 | 0.4093 (9) | 0.2421 (6) | 0.0851 (2) | C17 | 0.1800 (8) | 0.4626 (5) | 0.3199 (2) |
| C4 | 0.2515 (9) | 0.2992 (6) | 0.0580 (2) | C18 | 0.1645 (12) | 0.4969 (6) | 0.3810 (3) |
| C5 | 0.0918 (9) | 0.3306 (5) | 0.0885 (2) | C8 | −0.2882 (8) | 0.3765 (6) | 0.2630 (2) |
| C6 | 0.0840 (7) | 0.3101 (5) | 0.1492 (2) | C9 | −0.3262 (8) | 0.2805 (7) | 0.3086 (3) |
| C7 | −0.0847 (8) | 0.3443 (5) | 0.1804 (2) | | | | |

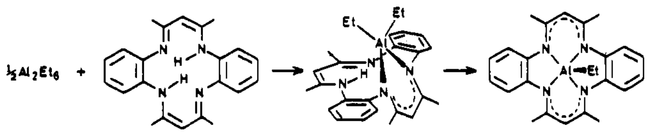

**Figure 1.** Insertion mechanism for Al($C_{22}H_{22}N_4$)$C_2H_5$.

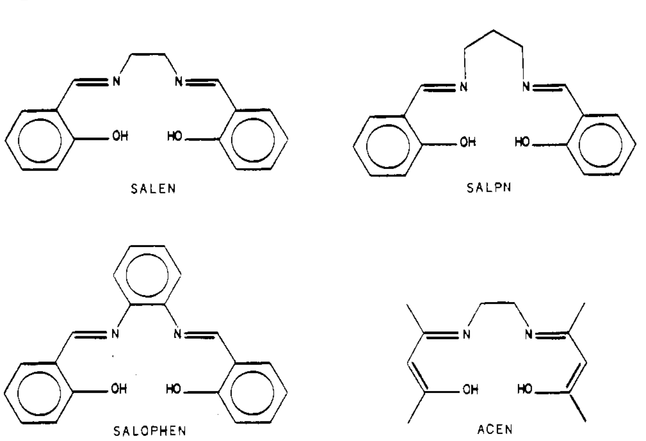

**Figure 2.** Schiff bases used in this study.

insertion was achieved by heating the solution at 75 °C for several hours. Colorless needles were formed on slow evaporation of the solvent.

**Physical Measurements.** Infrared spectra were recorded on a Perkin-Elmer 983 spectrometer between 4000 and 500 cm$^{-1}$ using NaCl plates and Nujol mulls. Proton NMR spectra were obtained on a Bruker-IBM 270-MHz instrument equipped with variable-temperature capabilities.

**Growth and Selection of X-ray Data Crystals.** Crystals of Al(SALEN)$C_2H_5$ were grown by slow cooling of the reaction mixture. A crystal approximately 0.35 × 0.35 × 0.40 mm$^3$ was selected and mounted on a thin glass fiber with epoxy resin for data collection.

**Collection and Reduction of X-ray Diffraction Data.** The diffraction data were obtained on an Enraf-Nonius CAD4 diffractometer controlled by a Digital PDP 11/34 computer with the use of graphite-monochromatized Mo K$\alpha$ radiation (λ = 0.71073 Å) at room temperature. Unit cell parameters were obtained from the indexing and least-squares refinement of 25 orientation reflections. The compound crystallizes in the orthorhombic crystal system, and the space group was uniquely determined by the systematic absences and found to be $P2_12_12_1$. The details of data collection are summarized in Table IA. Data were collected in the $+h,+k,+l$ octant. No corrections for absorption ($\mu$ = 1.294 cm$^{-1}$) or extinction were necessary.

**Solution and Refinement of the Structure.** The structure was solved by direct methods using MULTAN 78.[12a] Approximately 70% of the structure was observed on the first MULTAN attempt. The remaining non-hydrogen atoms were located from difference Fourier maps. The structure was refined by successive least-squares and Fourier techniques.[12b] The function minimized was $R_w = |\sum_i(w_i)|F_o - F_c|^2/\sum(w_iF_o^2)|$ where $w = 1/\sigma$. In the final refinement, anisotropic thermal parameters were used for all non-hydrogen atoms. Hydrogen atom positions were calculated by assuming idealized geometry and were included in structure factor calculations, but their parameters were not refined. The final weighted and unweighted $R$ indices are 6.3 and 4.7%, respectively. The final difference Fourier map was essentially featureless with no peaks greater than 0.28 e/Å$^3$. Table IB gives the positional parameters for the non-hydrogen atoms.

## Results and Discussion

**Synthesis and Characterization of Schiff-Base Aluminum Alkyl Complexes.** The Schiff-base aluminum alkyl complexes are easily synthesized by the addition of a stoichiometric amount of trialkylaluminum to the tetradentate bases having two replaceable protons. The reactions are exothermic; ethane and an aluminum alkyl ligand complex are produced immediately on mixing. Heat may be required to completely insert the monoalkylaluminum species. While ligand reduction instead of aluminum alkyl insertion was an early consideration, this has not been observed with any of the unsaturated ligands studied. Al(L)$C_2H_5$ where L = SALEN, SALOPHEN, SALPN, and ACEN have been prepared. These complexes have been characterized by $^1$H NMR spectroscopy in noncoordinating solvents. Table II summarizes the $^1$H NMR spectral data. The $^1$H NMR data indicate an inequivalence of the bridging methylene resonances for the SALEN, SALPN, and ACEN complexes. There is also only one vinylic resonance for each of these complexes. These data are consistent with the ligand adopting a square-planar geometry about the

---

(12) (a) Main, P. *MULTAN 78. A System of Computer Programs for the Automatic Solution of Crystal Structures from X-ray Diffraction Data*; Department of Physics, University of York: York, England, 1978. (b) All computations were performed on a PDP 11/34 computer with the aid of the Structure Determination Crystallographic Program Library, purchased with the Enraf-Nonius X-ray crystallographic system.

**Table II.** $^1H$ NMR ($\delta$) of Schiff-Base Aluminum Alkyl Complexes in $CDCl_3$

| | ACEN | SALEN | SALPN[a] | SALOPHEN |
|---|---|---|---|---|
| | 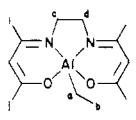 | 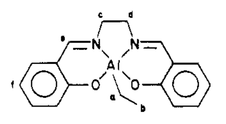 | 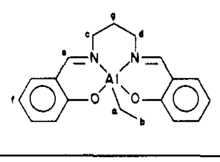 | 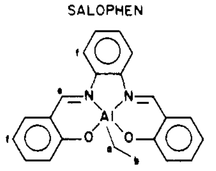 |
| a (q) | −0.43 | −0.33 | −0.15 | −0.40 |
| b (t) | 0.80 | 0.61 | 0.82 | 0.61 |
| c (m) | 3.28 | 3.67 | 3.47 | |
| d (m) | 3.34 | 4.00 | 3.80 | |
| e (s) | | 8.27 | 8.02 | 8.69 |
| f (m) | | 6.64–7.44 | 6.48–7.35 | 6.64–7.60 |
| g (m) | | | 1.79, 2.03 | |
| h (s) | 4.93 | | | |
| i (s) | 1.84 | | | |
| j (s) | 1.93 | | | |

[a] Benzene present in spectrum.

**Table III.** $^1H$ NMR Resonances ($\delta$) as a Function of Solvent

| | SALEN | | $Al[SALEN]C_2H_5$ | |
|---|---|---|---|---|
| | $C_6D_6$ | $CDCl_3$ | $C_6D_6$ | $CDCl_3$ |
| ethyl bridge | 3.20 | 3.97 | 2.95, 2.38 | 4.00, 3.67 |
| benzenoid | 6.4–7.3 | 6.8–7.4 | 6.5–7.2 | 6.6–7.5 |
| vinyl H | 7.75 | 8.34 | 7.26 | 8.27 |
| O–H | 13.40 | 13.65 | | |
| $CH_2$ alkyl | | | 0.19 | −0.33 |
| $CH_3$ alkyl | | | 1.30 | 0.61 |

aluminum. The ethyl group completes the aluminum coordination sphere, binding in the axial position. This square-pyramidal geometry of the aluminum center accounts for both the equivalence of the vinylic hydrogens and the inequivalence of the methylene bridging groups. A trigonal-bipyramidal structure would not have both equivalent vinylic and inequivalent methylene resonances. This square-pyramidal coordination geometry is also found in the solid state for the SALEN complex (vide infra). The Al–ethyl resonances for these complexes all occur above 1.0 ppm. The chemical shifts of the alkyl group are dependent on a variety of factors, particularly deshielding effects from the aromatic rings of the ligands. Our attempts to correlate chemical shifts or $\Delta = \nu_{CH_3} - \nu_{CH_2}$ with Al–C bond polarity were unsuccessful. The $^1H$ NMR resonances for these complexes as well as the free ligands are strongly solvent-dependent. Table III summarizes the $^1H$ NMR data in $CDCl_3$ and $C_6D_6$ for SALEN.

**Reactivity of Al(Schiff base)$C_2H_5$ Complexes.** Once isolated, the aluminum Schiff-base alkyl complexes exhibit an aluminum–ethyl bond reactivity intermediate between that observed for aluminum macrocyclic alkyl complexes and trialkylaluminates. This reactivity varies markedly for the Schiff-base ligands investigated. Although these ligands have the same donor atoms and similar chemical behavior, this difference in reactivity appears to be dependent on the flexibility of the "backbone" connecting the salicylaldehyde chelates.

This is clearly demonstrated in the hydrolysis of the salicylaldehyde-derived base series. Of the ligands investigated, SALOPHEN is the most rigid because it is totally conjugated, and SALPN is the least rigid. SALPN, with its three fused 6-membered chelate rings, also does not present as good a square-planar coordination geometry as the other ligands but tends to twist into a distorted geometry. In 0.01 M complex solutions in chloroform with a 2–3-fold excess of water, hydrolysis of the SALOPHEN complex is extremely slow. Less than 5% of the complex had reacted after 2 days. For the more flexible SALEN and SALPN complexes, the relative rates of hydrolysis were significantly faster. The half-life for the rate of disappearance of the SALEN complex is 30 min at room temperature while that of the SALPN complex under similar conditions was less than 9 min.

The greater stability of the SALOPHEN complex is also demonstrated by its reactivity with weak acids. Addition of a 100-fold excess of acetic acid to a 0.01 M Al(SALOPHEN)$C_2H_5$ solution in chloroform results in the slow formation of the Al(SALOPHEN)OAc complex. Complete protonolysis of the ethyl group producing ethane takes 45 min. In contrast, addition of acetic acid to Al(SALEN)$C_2H_5$ under similar conditions results in the instantaneous formation of the acetate complex and ethane. With a stronger acid such as hydrochloric or perchloric acid, protonolysis occurs immediately on addition for all of the complexes studied. The greater stability of the SALOPHEN complex approaches that seen for the macrocyclic $Al(C_{22}H_{22}N_4)C_2H_5$ complex.[7]

**Table IV.** Comparison of Al(SALEN)$C_2H_5$ and $[Al(SALEN)]_2O$ $^1H$ NMR Resonances ($\delta$)

| | | 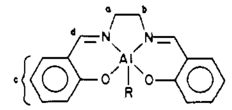 | |
|---|---|---|---|
| | | Al(SALEN)$C_2H_5$ | $[Al(SALEN)]_2O$ |
| methylene | a | 3.57 | 3.38 |
| | b | 4.00 | 3.92 |
| benzene | c | 6.70 | 6.62 |
| | | 7.09 | 6.98 |
| | | 7.38 | 7.26 |
| vinyl | d | 8.27 | 7.79 |

All these complexes are resistant to atmospheric hydrolysis in the solid state. Crystals of the SALEN and SALOPHEN compounds show no evidence of decomposition after 6 months. All the complexes react immediately with HCl in the solid state, producing the chloro Al(Schiff base) complex.

Hydrolysis of the aluminum ethyl complexes in moist solvents produces the insoluble hydroxo Al(Schiff base) complexes. If the solution is heated in the presence of unreacted alkyl complex, the $\mu$-oxo ligand species is formed. In the presence of excess water, the equilibrium shifts back to the formation of the hydroxo species as monitored by $^1H$ NMR. The $\mu$-oxo and hydroxo complexes have been isolated for Al(SALEN) and characterized by infrared spectroscopy. The hydroxo complex features a very weak IR absorption at 3588 cm$^{-1}$, assigned to the OH stretching frequency. The Al–O stretching frequency cannot be definitively assigned due to the complicated ligand absorption modes. The $\mu$-oxo spectrum shows a strong absorption at 1067 cm$^{-1}$, assigned to the asymmetric Al–O–Al stretching mode. This is comparable to the 1052-cm$^{-1}$ frequency reported for the $\mu$-oxo Al(phthalocyanine) dimer[13] and higher than the 997-cm$^{-1}$ frequency observed for the $\mu$-oxo $Al(C_{22}H_{22}N_4)$ dimer.[7] The crystal structure[14] for the $\mu$-oxo Al(phthalocyanine) dimer shows a very short Al–O bond, 1.679 (2) Å, consistent with the high-frequency Al–O–Al stretching mode. The Al–O distance in the $\mu$-oxo Al(SALEN) complex is also expected to be quite short.

---

(13) Owen, J. E.; Kenney, M. E. *Inorg. Chem.* **1962**, *1*, 334.
(14) Wynne, K. J. *Inorg. Chem.* **1985**, *24*, 1339.

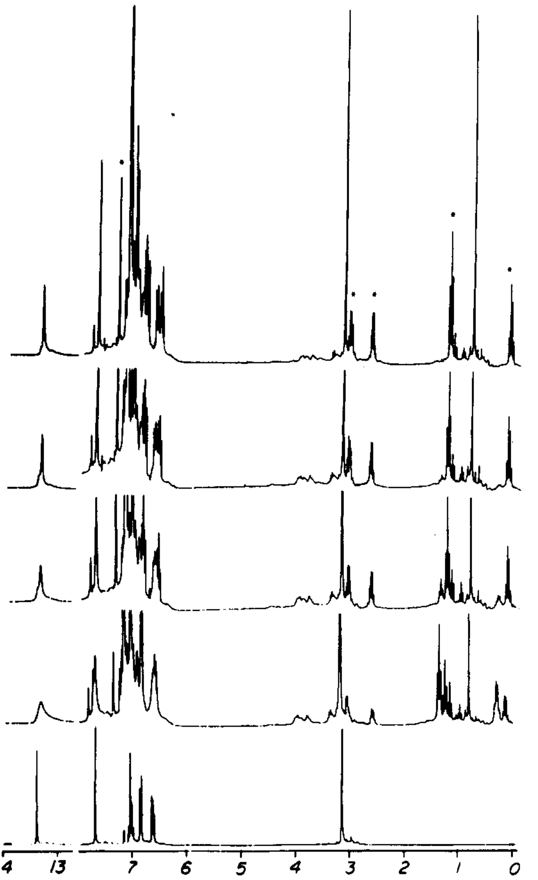

**Figure 3.** $^1H$ NMR spectra monitoring Al–$C_2H_5$ insertion in SALEN. The asterisks indicate inserted product peaks with the exception of the benzenoid resonances.

The $\mu$-oxo Al(SALEN) complex has also been characterized by $^1H$ NMR spectroscopy. The $^1H$ NMR resonances of the ligand protons for the $\mu$-oxo Al(SALEN) dimer and for Al(SALEN)$C_2H_5$ are presented in Table IV. The dimer resonances are shifted upfield from those observed for the monomer. This greater shielding of the dimer resonances is attributed to ring current effects between the aromatic rings of the cofacial SALEN species. No $^1H$ NMR results are available for the hydroxo complex because of its insolubility in organic solvents.

All the Schiff-base compounds investigated are stable to $\beta$-elimination under the conditions of formation, which require prolonged heating at 85 °C in some cases. Heating to higher temperatures results in ligand decomposition with no evidence for the formation of ethene. Also, because of the lack of intense chromophores in these complexes, photolytic dissociation of the Al–C bond was not observed. The intensely colored alkylaluminum complexes of macrocyclic and porphyrin ligands are quite photosensitive and undergo homolytic Al–C bond cleavage.[6,7]

**Solution $^1H$ NMR Studies.** The solution chemistry of the reaction of triethylaluminum with the Schiff-base ligands was studied in order to identify the long-lived intermediates existing prior to insertion. Two different insertion mechanisms may be operating in these systems: one for the salicylaldehyde ligands and another for ACEN. While both mechanisms are stepwise, the one actually followed by these ligands may depend on both the acidity of the replaceable hydroxyl protons and the flexibility of the ligand environment. The protons on the ligands derived from salicylaldehyde are more acidic than ACEN's, and the ligands themselves are more bulky due to the benzene rings.

**Mechanism for Salicylaldehyde-Derived Ligands.** The insertion reaction with these ligands is most rapid for SALOPHEN and slowest for SALPN, indicating a strong dependence on the length of the bridging linkage. The acidity of the phenolic OH's does not vary considerably for this series. The rate of insertion is solvent-dependent: for example, it occurs much more rapidly in chloroform than in benzene. For the SALEN complex, insertion in chloroform was complete within 3 min. In benzene, the insertion required approximately 20 min and thus was readily followed via $^1H$ NMR spectroscopy. These spectra are shown in Figure 3. The bottom spectrum is that of the free ligand. In the second spectrum less than a stoichiometric amount of $Al(C_2H_5)_3$ has been added, and the third through fifth spectra monitor the insertion. On the basis of these $^1H$ NMR results the mechanism depicted in Figure 4 is suggested.

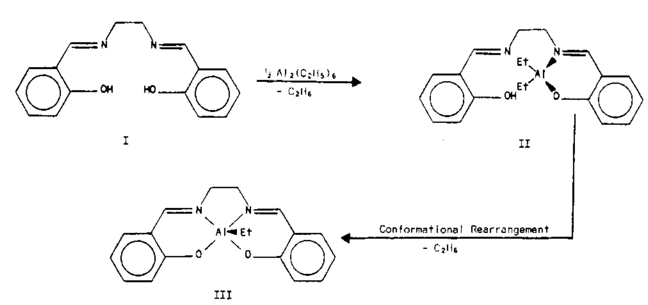

**Figure 4.** Proposed mechanism for Al insertion in the salicylaldehyde-derived ligands.

The first step involves the reaction of triethylaluminum with one of the hydroxyl protons, producing ethane and the bisadduct, II. This is shown clearly in the $^1H$ NMR spectra. On addition of triethylaluminum to SALEN, new vinylic hydrogen peaks at 7.8 and 7.9 ppm appear, corresponding to the two different peaks expected for the bisadduct. Splitting of the hydroxyl resonance at 13.3 ppm indicates the formation of a new hydroxyl species. Also, new peaks between 3.0 and 4.2 ppm are attributable to the methylene peaks of the bisadduct. The peak at 0.8 ppm is attributable to ethane formation. The loss of the first ethyl group and the concomitant coordination of the diethylaluminum species to the oxygen and nitrogen of the salicylidene moiety stabilizes, to some extent, the remaining two aluminum–alkyl bonds. These groups are still quite reactive, and the remaining hydroxyl proton is sufficiently acidic that, with time and ligand conformational rearrangement (if necessary), the second hydroxyl proton reacts with an ethyl group, forming ethane and the inserted monoethylaluminum ligand complex, III. In the $^1H$ NMR spectra, the peaks attributed to species II gradually disappear and are replaced by those of the completely inserted product. This two-step insertion process is similar to that observed for the $C_{22}H_{22}N_4{}^{2-}$ complex[7] mentioned earlier.

Of the three salicylaldehyde-derived ligands studied, insertion is most rapid for SALOPHEN. Insertion occurs almost instantaneously. The SALPN complex is the most difficult to synthesize; heating is required to achieve insertion. The increased difficulty in insertion for the more flexible ligands is attributed to steric factors. With these very similar ligands, the salicylidene N–O bite is the same, but the propyl linkage probably causes a distortion of the coordination sphere from ideality. Molecular models indicate a distorted twisted geometry that may impose a barrier to the final reaction that involves the neutralization of the remaining hydroxyl proton and the loss of the second ethyl group. The SALOPHEN ligand, as a result of its planar configuration, requires no conformational rearrangement with respect to the bridging unit; the insertion has a low activation barrier and occurs rapidly.

**Mechanism and Solution Studies for ACEN.** As stated, the reaction of $Al(C_2H_5)_3$ with ACEN follows a different path than for the salicylaldehyde-derived ligands. When a stoichiometric amount of aluminum alkyl is added to the ligand in benzene, the resulting $^1H$ NMR spectrum is complicated and indicates a mixture of products. To better understand this system, the reaction of $Al(C_2H_5)_3$ with ACEN was investigated for several metal to ligand ratios.

**4:1 Adduct.** Addition of 4 equiv of $Al(C_2H_5)_3$ to 1 equiv of ACEN produces ethane and a solution species whose $^1H$ NMR and structure are depicted in Figure 5. Two $Al(C_2H_5)_3$ molecules are involved in a donor–acceptor complex with the ACEN nitrogen

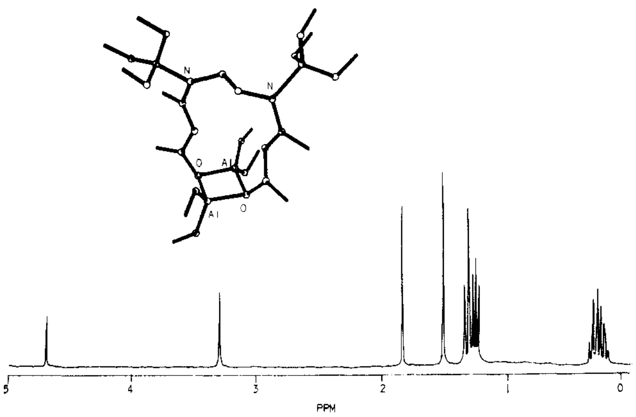

**Figure 5.** $^1$H NMR spectrum of the 4:1 adduct.

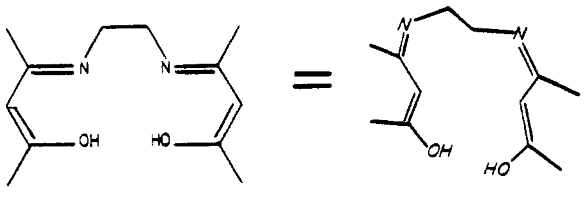

**Figure 6.** Ligand conformations for ACEN.

atoms. Reaction of each ACEN hydroxyl group with a $Al(C_2H_5)_3$ complex leads to the formation of ethane and a 4-membered Al–O ring. Each aluminum is tetrahedrally coordinated to two ethyl groups and to the two bridging hydroxyl oxygens. The ACEN ligand adopts an "inverted" configuration as compared to its usual planar structure. This is depicted in Figure 6. The integrated intensity of the peaks and the spectral features are consistent with the proposed structure. Expansion of the region between 1.0 and 1.5 ppm reveals that the multiplet centered at 1.32 ppm is actually two overlapping triplets. The upfield triplet has two-thirds the intensity of the downfield triplet and thus is assigned to the ethyl groups of the 4-membered Al–O ring. The multiplet due to the methylene quartets between 0.5 and 0.0 ppm is even more complicated. Inspection of the expanded region reveals the expected two overlapping quartets. The upfield quartet, however, is actually a doublet of quartets equal in intensity. The less intense upfield quartets are assigned to the ethyl groups of the 4-membered ring. This splitting is consistent with the proposed structure in that the environments above and below the 4-membered ring are different. (See Figure 5.) Any sort of linear structure would allow free rotation of the diethylaluminum moiety, and thus no splitting of the methylene resonance would be observed. Also, a linear structure would feature a very reactive, coordinatively unsaturated aluminum center and is thus unlikely. In other structures with potentially coordinatively unsaturated aluminum–oxygen bonds, the molecules dimerize, forming a 4-membered Al–O bridging unit.[15] Molecular models indicate that the geometry of ACEN is such that the complex can form a cyclic structure as proposed, instead of dimerizing with another ACEN molecule to remove the coordinative unsaturation.

**2:1 Adduct.** When a twofold excess of $Al(C_2H_5)_3$ is added to ACEN, ethane is produced and the solution warms. The $^1$H NMR spectrum is shown in Figure 7. The integrated intensities of the absorptions are consistent with any of the three solution species presented in Figure 8. While all fulfill the stoichiometric requirements, structure VI is the most probable and is consistent with the oxophilic character of aluminum. Structure VI is most similar to the 4:1 adduct previously proposed. The chemical shifts due to ligand protons differ only slightly. Structures IV and V provide a markedly different chemical environment for the ligand protons, and if the 2:1 adduct were either of these structures, one would expect a greater variation in chemical shifts as compared to the 4:1 adduct. Structure IV is also considered unlikely due to the known (vide infra) difficulty in aluminum insertion with this ligand and the improbability of having both four- and six-coordinate aluminum centers in the same complex.

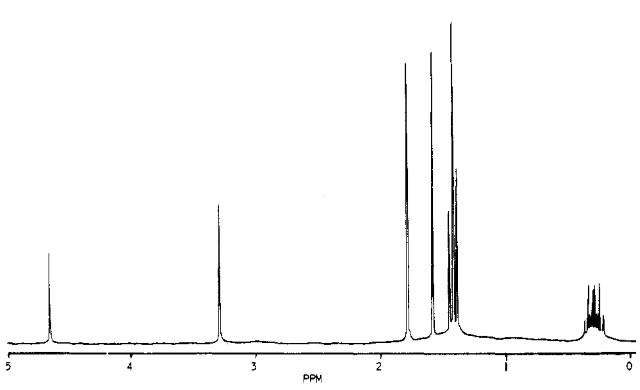

**Figure 7.** $^1$H NMR spectrum of the 2:1 adduct.

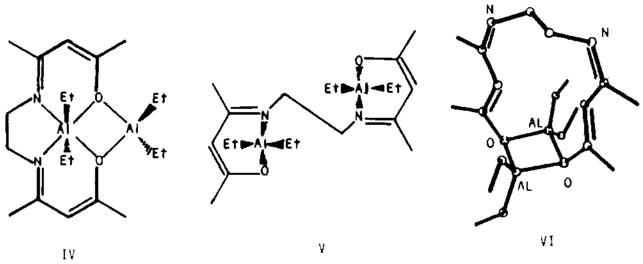

**Figure 8.** Possible structures for the 2:1 adduct.

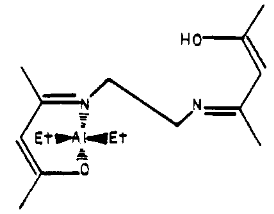

**Figure 9.** Proposed half-inserted 1:1 complex.

**1:1 Adduct.** As stated previously, the spectrum due to the 1:1 adduct is very complicated. Observed resonances correspond to both the 2:1 complex and the free ligand. There are also resonances assigned to an inserted and half-inserted 1:1 complex. The half-inserted complex is suggested to have the structure given in Figure 9. When the 1:1 solution mixture is allowed to stand, the resonances attributed to the free ligand, the 2:1 complex, and the 1:1 half-inserted complex slowly disappear and those due to the inserted monoethyl complex appear. This process is hastened by heating. The observed 1:1 solution spectrum was surprising in that the insertion mechanism differs from that observed for SALEN. One would have expected to see primarily the 1:1 half-inserted adduct. Also, the existence of a 2:1 adduct in the presence of free ligand was unexpected.

The mechanism depicted in Figure 10 accounts for the observed $^1$H NMR spectra. In this case, the reaction stoichiometry may be considered to be $^1/_2Al_2(C_2H_5)_6$ to one ACEN unit rather than one $Al(C_2H_5)_3$ to one ligand unit, as was seen for the salicylaldehyde ligands. The mechanism is still stepwise. In the first step, one hydroxyl proton reacts with the bridging ethyl unit of the triethylaluminum dimer. The oxygen is then bound to both aluminum centers, and ethane is produced. In a second step, the other hydroxyl proton interacts with the remaining bridging ethyl moiety and a 4-membered Al–O ring is formed. Thus, for ACEN, the dimeric nature of triethylaluminum is preserved. Complete insertion requires the breakup of the stable Al–O ring and the subsequent migration of aluminum ethyl species to the unreacted free ligand. Thus, the insertion is a multicentered reaction process and is much more complicated than for SALEN. The activation energy for insertion is higher, and the process is thus facilitated by heat.

---

[15] Kai, Y.; Yasuoka, N.; Kasai, N.; Kukudo, M.; Yasuda, H.; Tani, H. *J. Chem. Soc. D* **1969**, 575.

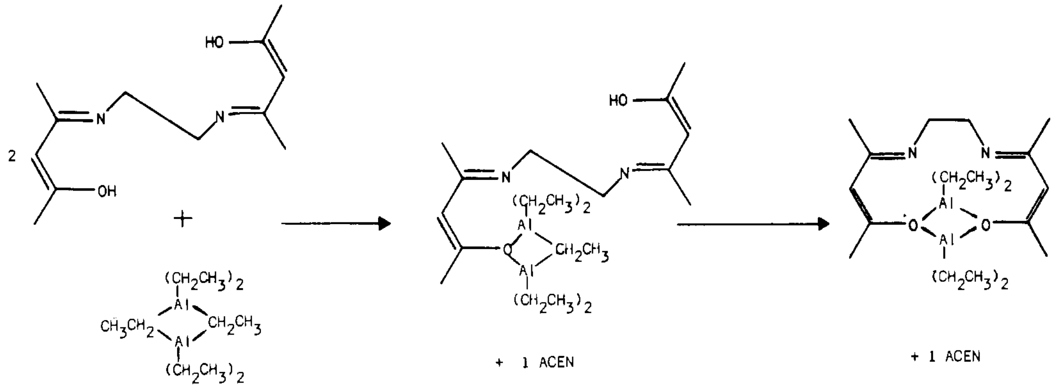

Figure 10. Proposed mechanism for Al insertion in ACEN.

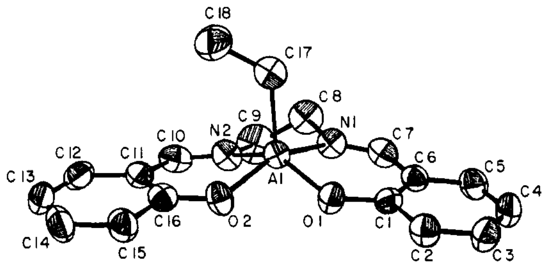

Figure 11. Perspective view and labeling scheme of $Al(SALEN)C_2H_5$ with 50% probability ellipsoids.

Table V. Bond Distances (Å) for $Al[SALEN]C_2H_5$

| bond | dist | bond | dist |
|---|---|---|---|
| Al-O1 | 1.800 (5) | N1-C8 | 1.501 (9) |
| Al-O2 | 1.829 (5) | C8-C9 | 1.460 (10) |
| Al-N1 | 2.013 (6) | C9-N2 | 1.507 (9) |
| Al-N2 | 2.027 (6) | N2-C10 | 1.256 (8) |
| Al-C17 | 1.966 (7) | C10-C11 | 1.429 (8) |
| O1-C1 | 1.321 (6) | C11-C12 | 1.429 (9) |
| C1-C2 | 1.404 (7) | C12-C13 | 1.342 (10) |
| C2-C3 | 1.384 (8) | C13-C14 | 1.345 (10) |
| C3-C4 | 1.388 (9) | C14-C15 | 1.396 (9) |
| C4-C5 | 1.351 (9) | C15-C16 | 1.420 (7) |
| C5-C6 | 1.418 (8) | C16-C11 | 1.387 (7) |
| C6-C7 | 1.416 (7) | C16-O2 | 1.306 (7) |
| C1-C6 | 1.418 (7) | C17-C18 | 1.459 (10) |
| C7-N1 | 1.268 (7) | | |

**2:1 Inserted Adduct.** On addition of 1 equiv of $Al(C_2H_5)_3$ to 1 equiv of inserted $Al(ACEN)C_2H_5$, the solution warms and turns orange. Spectra taken within 10 min of addition show a coalescence of the bridging methylene resonances and the growth of 2 quartets centered at 0.45 and 0.05 ppm. These observations are consistent with the formation of species IV shown in Figure 8 for the 2:1 adducts. As expected, this species is extremely reactive and ligand decomposition rapidly takes place. This decomposition is facilitated by heat.

**Description of the Structure of $Al(SALEN)C_2H_5$.** The crystal structure of $Al(SALEN)C_2H_5$ consists of a 5-coordinate square-pyramidal $Al^{3+}$ strongly bound to both the oxygen and nitrogen ligand atoms. Figure 11 shows a view of the molecule with the atom designations. The SALEN ligand has the typical "inverted umbrella" geometry seen for some monomeric trivalent transition-metal SALEN complexes.[16] The ethyl bridge is rigid, one methylene carbon above and one below the plane of the nitrogen and oxygen donor atoms. The ethyl group is staggered with respect to the N and O of a salicylidene moiety and away from the methylene carbon. Selected interatomic distances and angles are listed in Tables V and VI, respectively.

**Coordination Geometry.** The Al–C distance of 1.966 (7) Å is similar to the terminal Al–C distance of 1.970 Å observed for $Al_2(CH_3)_6$[17] and that of 1.976 (3) Å observed for the 5-coordinate macrocyclic complex $Al(C_{22}H_{22}N_4)C_2H_5$[7] but is shorter than the distance of 2.01 (1) Å observed for $[Al(cyclam)(ClO_4)_2C_2H_5]\text{-}CH_3CN$.[8] This indicates a strong Al–C bond.

Table VI. Bond Angles (deg) for $Al[SALEN]C_2H_5$

| bond seq | angle | bond seq | angle |
|---|---|---|---|
| O1-Al-O2 | 88.4 (3) | Al-C17-C18 | 120.2 (6) |
| O1-Al-N1 | 88.1 (3) | O1-Al-C17 | 112.9 (3) |
| O1-Al-N2 | 142.1 (3) | O2-Al-C17 | 107.3 (3) |
| O2-Al-N1 | 151.1 (3) | N1-Al-C17 | 100.5 (3) |
| O2-Al-N2 | 86.1 (3) | N2-Al-C17 | 104.5 (3) |
| N1-Al-N2 | 79.3 (3) | | |

Table VII. Comparison of Al–O Bond Distances (Å) in Organoaluminum Compounds

| | |
|---|---|
| $[Me_2AlOC(Ph)N(Ph)]ONMe_3$ | 1.77 (7), 1.815 (8) |
| $K[AlMe_2(OPh)_2]$ | 1.79 (2) |
| $[NMe_4]AlMe_3(Me(oo))]$ | 1.83 (1) |
| $AlMe_2(ONNMeO)AlMe_3$ | 1.881 (6), 1.909 (6), 2.004 (6) |
| $[AsMe_4][AlMe_2OAlMe_3]_2$ | 1.78 (2), 1.80 (2) |
| $[Me_2AlOMe]_3$ | 1.851 (3) |
| $[Me_2AlOC(Ph)N(Ph)\cdot MeCHO]_2$ | 1.868 (6), 1.966 (6), 2.047 (7) |

The average Al–N distance of 2.020 (7) Å is identical with the Al–N distance in the 4-coordinate $CH_3CN\cdot Al(CH_3)_3$ Lewis adduct[18] and the average Al–N cyclam distance in the 6-coordinate cyclam complex[8] but is longer than the 1.967 (3) Å distance in the $C_{22}H_{22}N_4$ complex. The average Al–O distance of 1.815 (15) Å is shorter than that of the Al–N bonds, consistent with the oxophilicity of aluminum. This distance is within the range of Al–O bonds presented in Table VII.[19]

The aluminum is displaced 0.540 Å from the best least-squares plane containing the chelating nitrogen and oxygen atoms. This displacement is larger than that observed for the cyclam complex (0.295 Å)[8] and for the 5-coordinate Al(phthalocyanine)Cl complex (0.410 Å)[20] but is slightly smaller than the 0.57-Å displacement seen for the $C_{22}H_{22}N_4$ complex.[7] The large out-of-plane distance for the SALEN complex is unexpected as the SALEN ligand is considerably more flexible than either $C_{22}H_{22}N_4$ or phthalocyanine.

**Comparison of the Structure with Transition-Metal SALEN Complexes.** The geometry of $Al(SALEN)C_2H_5$ is similar to a variety of related transition-metal SALEN complexes and is most similar to iron SALEN species. The average metal–oxygen and metal–nitrogen bond distances for a variety of di- and trivalent first-row transition-metal complexes are 1.904 and 1.912 Å, respectively, as reported by Calligaris and co-workers. The ranges for these values are 0.143 and 0.282 Å, respectively.[16] The Al–N and Al–O distances fall within this range.

The 0.540-Å displacement observed for the Al(SALEN) complex is significantly greater than for all of the transition-metal

---

[16] Calligaris, M.; Nardin, G.; Randaccio, L. *Coord. Chem. Rev.* **1972**, *7*, 385.

[17] Vranka, R. G.; Amma, E. L. *J. Am. Chem. Soc.* **1967**, *89*, 3121.

[18] Atwood, J. L.; Seale, S. K.; Robert, D. H. *J. Organomet. Chem.* **1973**, *51*, 105.

[19] Atwood, J. L.; Hrncir, D. C.; Shakir, R.; Dalton, M. S.; Priester, R. D.; Roger, R. D. *Organometallics* **1982**, *1*, 1021 and references therein.

[20] Wynne, K. J. *Inorg. Chem.* **1984**, *23*, 4658.

complexes with the exception of the iron compounds. The transition-metal ionic radii are all slightly larger than $Al^{3+}$, and thus the large displacement of aluminum is not the result of purely steric considerations. The structural features for the other Schiff-base aluminum alkyl complexes are expected to be similar to those for $Al(SALEN)C_2H_5$.

## Conclusions

Aluminum alkyl complexes with tetradentate Schiff bases of the type Al(Schiff base)$C_2H_5$ have been synthesized and found to have stabilities comparable to those of transition-metal complexes. Some of the long-lived solution intermediates prior to insertion have been identified. The reaction of $Al_2(C_2H_5)_6$ with tetradentate Schiff bases occurs stepwise. Two different mechanisms prevail depending on ligand properties. With ACEN, a quasi-stable four-membered Al–O ring is formed initially. This then reacts with excess ligand, producing the inserted $Al(ACEN)C_2H_5$ complex. With the salicylaldehyde-derived ligands, reaction first occurs with one of the hydroxyl protons, producing a half-inserted aluminum diethyl species. This in turn reacts with the remaining hydroxyl proton, releasing a second molecule of ethane and the inserted aluminum ethyl complex. All of the aluminum ethyl Schiff-base complexes exhibit 5-coordinate geometry about the aluminum center. The aluminum–carbon bond in these complexes is more reactive than in the tetraaza macrocycles[6-8] but less reactive than in complexes with mono- and bidentate ligands such as 8-hydroxyquinoline.[21] The bond length of the Al–C bond in SALEN is slightly shorter than for those of the macrocyclic complexes; thus, the lessened stability for $Al(SALEN)C_2H_5$ is probably due to kinetic rather than thermodynamic considerations.

Comparison of the hydrolysis tendencies of trivalent transition-metal alkyl complexes such as well-known Cr(III) and Co(III) species with analogous Al–alkyl complexes leads to some interesting conclusions. First of all, hydrolysis of a metal–carbon bond by a proton should be a straightforward process and to a first approximation be largely dependent upon the polarity of the M–C bond; i.e., the more polar, the more readily it is attacked by $H^+$. A second contribution to the overall energetics of this process is the energy of the dealkylated metal species remaining and the reorganizational energy required to achieve the ground-state conformation.

For the series of Al(Schiff base)$C_2H_5$ complexes examined in this report, the similarity of the coordination spheres of the tetradentate ligands would not be expected to lead to substantial differences in the polarity of the Al–C bond. Yet, a considerable range of rates is observed. These appear to correlate strongly with the degree of flexibility of the tetradentate ligand. The incredible stability of the previously reported macrocyclic aluminum alkyl complexes[7,8] and the surprisingly robust nature of the tetradentate Al–C complexes reported here are probably best accounted for with the following explanation.

Simple protonation of the carbon atom of an aluminum alkyl to produce the corresponding alkane should be a highly thermodynamically and kinetically favored process. However, in the absence of strongly coordinating anions (particularly oxo donors, which are not present in appreciable concentrations in acidic solutions), loss of the alkyl group will leave a four-coordinate square-planar intermediate. However, all known four-coordinate $Al^{3+}$ complexes are approximately tetrahedral. For a third-row metal, the d orbitals are relatively high in energy, such that suitable hybridization schemes for square-planar $Al^{3+}$ coordination are not available. However, if the Schiff base has a flexible backbone allowing facile coordination geometry rearrangements toward tetrahedral or distorted tetrahedral, the overall hydrolysis process may be more energetically favorable. In the case of transition-metal complexes, the greater d-orbital participation in the bonding leads to lower energy square-planar intermediates. Square-pyramidal geometry for $Al^{3+}$ is not as common as for transition metals; there are no known examples of stable square-pyramidal monoalkylaluminum complexes with mono- and bidentate ligands. The bis(acetylacetonate)alkylaluminum complex disproportionates to the mono and tris complex,[22] and work in our laboratory with 8-hydroxyquinoline alkyl complexes also indicates that the bis species is unstable.[21] In these systems, there are few if any constraints on the coordination geometries with a $d^0$ system such as $Al^{3+}$; a trigonal-bipyramidal structure is expected to be preferred over a square-pyramidal one. Factors affecting the stability of Al–C bonds should also be applicable to aluminum hydride systems. These are currently under investigation in our laboratories.

**Registry No.** $Al(SALEN)C_2H_5$, 102630-64-8; $Al(SALOPHEN)C_2H_5$, 102630-65-9; $Al(SALPN)C_2H_5$, 102630-66-0; $Al(ACEN)C_2H_5$, 102630-67-1; $Al(C_2H_5)_3$, 97-93-8; SALEN, 94-93-9; SALOPHEN, 3946-91-6; SALPN, 120-70-7; ACEN, 52751-14-1; $Al_4(SALEN)(C_2H_5)_{10}$, 102648-65-7; $Al(SALEN)(C_2H_5)_2$, 102630-68-2; $Al_2(SALEN)(C_2H_5)_4$, 102630-69-3.

**Supplementary Material Available:** Tables of anisotropic temperature factors, calculated hydrogen coordinates, and least-squares-plane calculations (3 pages). Ordering information is given on any current masthead page.

---

(21) Dzugan, S. J.; Goedken, V. L., to be submitted for publication.

(22) Kroll, W. R.; Naegele, W. *J. Organomet. Chem.* **1969**, *19*, 439.

---

Contribution from the Department of Chemistry,
University of Florida, Gainesville, Florida 32611

# Trans Influence across a Rh–Rh Bond. Effect of a Series of Lewis Bases on the Stretching Frequency of Coordinated CO

Carl Bilgrien, Russell S. Drago,* Glenn C. Vogel,[1] and James Stahlbush

*Received September 4, 1985*

The dependence of $\nu_{CO}$ upon $\sigma$-donor strength of the Lewis base B in $BRh_2(pfb)_4CO$ adducts, where pfb is perfluorobutyrate, has been probed. The systematic dependence of $\nu_{CO}$ upon the strength of the interaction of B with one rhodium center illustrates the ability of the metal–metal bond to transmit the influence of coordination of B to the second metal center and, hence, to the coordinated CO. It is found that $\nu_{CO}$ is well described by an *E* and *C* analysis that takes into account the inductive influence of trans base coordination. The deviation observed when B is a $\pi$-acceptor base is consistent with an earlier claim that metal–metal bonding in the $Rh_2^{4+}$ unit polarizes the d orbitals with $\pi$ symmetry, enhancing $\pi$-back-bonding interactions with donors that can also function as $\pi$ acceptors.

The CO ligand is ubiquitous in organometallic chemistry, and considerable effort has been put forth to understand the nature of M—C≡O bonding and the influence of various ligands upon the reactivity and spectroscopic properties of carbonyls. In probing

0020-1669/86/1325-2864$01.50/0